

Study on Micro Structural Properties of Sodium in Na₂O - Doped SiO₂ Melt using Molecular Dynamics Simulation

Abstract. Molecular dynamics (MD) simulation could provide details about local microstructure at atomic level, so we use this method to investigate micro-structural properties of sodium in Na₂O-doped SiO₂ melt. Additionally, we calculated the Voronoi polyhedrons to determine the spatial distribution of atoms in the simulation models. The result shows that many bridging oxygen (BO) polyhedrons and all Si-polyhedrons do not contain Na atoms. Most non-bridging oxygen (NBO) polyhedrons contain 2, 1 or no Na atoms, where BO, NBF is the O bonded with 2 and 1 or no Si, respectively. Average volume per polyhedron decreases in order: NBF_x-polyhedron → BO_x-polyhedron → Six-polyhedron. Na atoms are found in NBF_x-polyhedrons and frequently move through them leading to very fast diffusivity of Na in comparison with Si and O. The simulation shows that the number of neighbors around the NBF_x-polyhedron is larger than that around the BO_x-polyhedron.

Keywords: Na₂O-doped SiO₂, sodium, Voronoi polyhedron, micro-structure, subnets.

1. Introduction

The micro-structure of silica (SiO₂) is an archetypal network-forming system containing SiO₄ tetrahedra. The addition of doped Na atoms generates non-bridging oxygen (NBO) in SiO₄. Consequently, the Na₂O-doped SiO₂ gives various anomalous properties which are essential for industrial applications, ceramics, and understanding the fundamentals of minerals [1-5]. The Na₂O-doped SiO₂ melt has been intensively investigated by experimental techniques including photoelectron spectroscopy, X-ray diffraction, in situ Raman spectroscopy and elastic neutron scattering, and various simulation techniques [6-11]. The addition of doped Na ions to pure SiO₂ melt leads to a decoupling of alkali diffusion and diffusive transport in the Si-O network [10-17]. Davidenko et al. in ref. [7] suggested that the distribution where the increasing alkali oxide content causes the homogeneous increasing disruption of Si-O network of pure SiO₂ is in conflict with highly nonlinear dependence of viscosity on alkali concentration. In accordance with studies [18-21], the pre-peak at 0.9 Å⁻¹ in the micro-structure factor measured experimentally for alkali silicates is evidence for the diffusion pathway.

Various experimental results found that the micro-structure of these silicates is found to comprise micro-regions with high sodium concentration. The two micro structural samples, the modified random network and the compensated continuous random network predict some clustering of alkali atoms in the silicate's microstructure [22-24].

The structure as well as applications of silica and sodium silicate have also been shown in references [25-27]. However, the spatial distribution of Na in the Na₂O-doped SiO₂ melt remains not fully clarified yet. Therefore, in present study, we focus on Na₂O-xSiO₂ melt (x = 1, 2, 3, 4) at pressure of 0.1 MPa and temperatures of 1573 K. Based on the features of pair radial

distribution function (PRDF), topographies of the Voronoi Ax- polyhedrons, and subnets Si-O in system.

2. Computational method

We conduct the MD simulation for NS_x, i.e. Na₂O-SiO₂ (NS1), Na₂O-2SiO₂ (NS2), Na₂O-3SiO₂ (NS3) and Na₂O-4SiO₂ melt at pressure of 0.1 MPa and temperature of 1573 K. The total number of particles in each system is approximately equal to 10,000. The interaction potentials used includes two- and three-body terms, which reproduce well the micro structural and transport properties of sodium silicates. The complete description of these potentials can be found elsewhere [4,28]. In order to collect the micro-structure and dynamics data we additionally run the simulation for 150 ps to produce 76 configurations separated by 2 ps. The structure is analyzed by PRDF and by the one determined separately for BO and NBF. Here BO, NBO and FO are the oxygen which is bounded respectively with two, one or no Si; both NBO and FO are denoted to NBF.

Si-BO subnet, Si- and O-centered Voronoi polyhedrons have been calculated for every system. It turns out that the simulation box is fully filled by those polyhedrons. Each Na is placed inside one among them. Several typical polyhedrons are shown in Figure 1. The following, A-centered polyhedron is called an Ax-polyhedron, where A is the Si, O, BO or NBF; *x* is the number of Na placed in A-centered polyhedron. We call that all Six-polyhedrons and a part of Ox-polyhedrons are A0-polyhedron type. Moreover, Na often moves between Ox-polyhedrons leading to very fast sodium diffusivity. Fig.1 illustrates the system comprising a large Si-O subnet. The Si-O subnet is defined as a subset of Si and BO connected by Si-O bonds, where BO is bonded with two Si, while Si is bonded with four O forming the SiO₄ unit.

3. Results and discussions

To check the value of the simulation samples, we compared the position of the first peak of PRDF with experimental data. Table 1 lists the interatomic distances obtained from simulation, and experimental data [29]. Although r_{SiNa} and r_{NaNa} show some discrepancies, the built models overall are consistent with the experiments. In particular, they reproduce the experimental data for r_{SiSi} , r_{SiO} , r_{OO} , and r_{NaO} .

Samples	r_{SiSi}	r_{SiO}	r_{OO}	r_{SiNa}	r_{ONa}	r_{NaNa}
NS1	3.10	1.60	2.60	3.00	2.20	3.25
NS2	3.10	1.60	2.60	3.30	2.25	3.50
NS3	3.10	1.55	2.60	3.35	2.25	3.65
NS4	3.10	1.60	2.60	3.40	2.25	3.60
Exp. [29]	3.05	1.62	2.62	3.50	2.29	2.6-3.05

Figure 2 shows the PRDF determined for BO-Na, NBF-Na and O-Na pairs. A clear peak is seen for the NBF-Na pair, with a significant increase in height from NS1 to NS4. The location of this peak is slightly different. For the BO-Na pair, the height of the first peak is much lower than for the NBF-Na pair. This result indicates that Na atoms are mostly located around NBF and

rarely near BO. Furthermore, the local sodium density in BO_x and NBF_x polyhedra changes strongly with SiO concentration. Unlike the NBF-Na pair, the first peak of the Si-Na pair is located at 3.0-3.6 Å, which is significantly larger than that of the NBF-Na pair. This means that Na is not in the Six-polyhedrons. These marks are consistent with the reports in refs. [1-6].

Figure 3 shows snapshots of the distribution of coordination units SiO_x and NaO_y in a model of Na₂O-3SiO₂ melt at a pressure of 0.1 GPa (here we only draw a part with size 6×20×20 Å³). Figure 3 indicates that the micro-structure of Na₂O-3SiO₂ melt comprises the coordination units SiO₄, and some NaO₄, NaO₅. From Figure 3, it can be seen that the distribution of coordination units SiO₄ is not uniform. Still, it tends to form clusters of SiO₄, and the coordination units SiO₄ tend to connect via a common oxygen atom to form subnet Si-O. Similarly, the coordination NaO₄ tends to connect to create a cluster of NaO₄, and the Na₂O-3SiO₂ melt only contains some coordination NaO₅. Therefore, the micro-structure of Na₂O-3SiO₂ melt is built up from the intermixture of the clusters SiO₄, NaO₄, NaO₅, and free Na.

Table 2 shows the average volume per polyhedron in descending order: NBF_x-polyhedron → BO_x-polyhedron → Six-polyhedron, and it slightly varies with SiO₂ content. We note that $\langle x_{\text{NBFx}} \rangle$ is significantly larger than $\langle x_{\text{BOx}} \rangle$. Moreover, $\langle x_{\text{BOx}} \rangle$ changes powerfully with SiO₂ content. This result shows that the spatial distribution of sodium is strongly heterogeneous. In particular, the most important Na atoms are located in NBF_x polyhedra with a total volume of 27.11–67.10% of the simulation box. In the system with lower SiO₂ content, more Na diffused into the BO_x-polyhedron.

Table 2. Characteristics of A_x-polyhedrons. Here $\langle v_{\text{Six}} \rangle$, $\langle v_{\text{BOx}} \rangle$ and $\langle v_{\text{NBFx}} \rangle$ is the average volume per Six-, BO_x- and NBF_x-polyhedron, respectively; V_{Six} , V_{BOx} , V_{NBFx} and V_{SB} is the volume occupied by Six-, BO_x-, NBF_x-polyhedrons and volume of simulation box, respectively; m_{NBF} , N_{Na} is the number of Na in NBF_x-polyhedrons and total number of Na, respectively.

System	$\langle v_{\text{Six}} \rangle, \text{Å}^3$	$\langle v_{\text{BOx}} \rangle, \text{Å}^3$	$\langle v_{\text{NBFx}} \rangle, \text{Å}^3$	$V_{\text{Six}}/V_{\text{SB}}$	$V_{\text{BOx}}/V_{\text{SB}}$	$V_{\text{NBFx}}/V_{\text{SB}}$	$m_{\text{NBF}}/N_{\text{Na}}$
NS1	8.13	20.12	30.41	0.0920	0.2370	0.6710	0.8682
NS2	7.96	20.25	31.45	0.1140	0.4369	0.4491	0.8081
NS3	7.94	20.37	31.96	0.1260	0.5379	0.3361	0.7909
NS4	7.94	20.44	32.45	0.1324	0.5965	0.2711	0.7798

Different Six-polyhedrons, Ox-polyhedrons either are polyhedrons with $x_{\text{Ox}} = 0$ or $x_{\text{Ox}} > 0$. As shown in Figure 4, the number of BO₀-polyhedrons increases from 78.1 to 95.8% with increasing SiO₂ content. Figure 4 shows that most BO_x-polyhedrons are BO₀ and BO₁ polyhedrons, while the most important NBF_x-polyhedrons are either NBF₀, NBF₁, and NBF₂ polyhedrons. In addition, the Na atoms are concentrated in the NBF_x-polyhedrons instead of being uniformly distributed in the Ox-polyhedrons. The obtained result makes it possible to propose a simple diffusion model. Consequently, Na moves from BO_x and NBF_x-polyhedron sites. Each slot is empty or occupied by one Na in BO_x-polyhedron, an NBF_x polyhedron has one and two points respectively. There are also torus polyhedrons with more than 2 sites, but their concentration is very low. Na transfer between Ox-polyhedrons results in very fast diffusion of Na compared to Si and O [10,20].

The sodium distribution in polyhedrons shown in Figure 5, it can be wide and asymmetrical. A pronounced peak is seen. This result confirms the fact that Na atoms are concentrated in NBF-polyhedrons instead of uniformly distributed through O-polyhedrons.

In summary, Na atoms are concentrated in NBF-polyhedrons instead of uniformly spreading through O-polyhedrons. The frequent displacing of Na between polyhedrons mainly contributes to the sodium's diffusion. The system consists of the NBO-FO, interfacial and Si-BO regions. The rate of $Ax \rightarrow Ax'$ happening in those regions reduces in the order: NBO-FO region \rightarrow interface region \rightarrow Si-BO region. Therefore, our results can propose that Na atoms diffuse by hopping alone and collective movement, but the major amount of Na moves collectively across O-polyhedrons located nearby. For melt with high SiO₂ content the NBO-FO region can represent the preferential sodium's diffusion pathway.

4. Conclusion

MD simulation is carried out for NS_x melt at temperature of 1573 K and pressure of 0.1 MPa. Micro-structural properties are investigated through Voronoi polyhedron. The result shows a pronounced peak for the NBF-Na pair of which the height varies with SiO₂ content. The position of the first peak for Si-Na peak is located at a distance significantly larger than that for the NBF-Na pair. The simulation demonstrates that Na atoms mostly present in the vicinity of NBF and rarely around BO. Simulation reveals that Na atoms are not placed in Six-polyhedrons and in about 32.9 to 72.89 % of total BO_x-polyhedrons. Most NBF_x-polyhedrons contain 2, 1 or no Na. The average volume per polyhedron decreases dramatically in the order: NBF_x-polyhedron \rightarrow BO_x-polyhedron \rightarrow Six-polyhedron. Although the average volume per polyhedron weakly depends on SiO₂ content, the volume occupied by all NBF_x-polyhedrons varies strongly with SiO₂ content. We also discovered that Na atoms are not only located in NBF_x-polyhedrons, but they also move frequently through them. Therefore, we suggest that melt with high SiO₂ content the NBO regions and FO regions can represent the preferential sodium's diffusion pathway.

Disclaimer (Artificial intelligence)

We hereby declare that NO generative AI technologies such as Large Language Models (ChatGPT, COPILOT, etc) and text-to-image generators have been used during writing or editing of manuscripts.

References

1. Zhong, Cong, et al. "Experimental characterizations and molecular dynamics simulations of the structures of lead aluminosilicate glasses." *Journal of Non-Crystalline Solids* 576 (2022): 121252.
2. Vargheese, K. Deenamma, Adama Tandia, and John C. Mauro. "Molecular dynamics simulations of ion-exchanged glass." *Journal of non-crystalline solids* 403 (2014): 107-112.
3. Yen, N. V., et al. "Spatial distribution of cations through Voronoi polyhedrons and their exchange between polyhedrons in sodium silicate liquids." *Journal of Non-Crystalline Solids* 566 (2021): 120898.

4. Saito, Yoshihiro, Takumi Yonemura, Atsunobu Masuno, Hiroyuki Inoue, Koji Ohara, and Shinji Kohara. "Structural change of Na₂O-doped SiO₂ glasses by melting." *Journal of the Ceramic Society of Japan* 124, no. 6 (2016): 717-720.
- [5] Tuheen, Manzila Islam, Lu Deng, and Jincheng Du. "A comparative study of the effectiveness of empirical potentials for molecular dynamics simulations of borosilicate glasses." *Journal of Non-Crystalline Solids* 553 (2021): 120413.
- [6] Bertani, Marco, et al. "Accurate and Transferable Machine Learning Potential for Molecular Dynamics Simulation of Sodium Silicate Glasses." *Journal of Chemical Theory and Computation* 20.3 (2024): 1358-1370.
- [7] Davidenko, A. O., V. E. Sokol'skii, A. S. Roik, and I. A. Goncharov. "Structural study of sodium silicate glasses and melts." *Inorganic Materials* 50, no. 12 (2014): 1289-1296.
- [8] Zhao, Qing, Michael Guerette, Garth Scannell, and Liping Huang. "In-situ high temperature Raman and Brillouin light scattering studies of sodium silicate glasses." *Journal of non-crystalline solids* 358, no. 24 (2012): 3418-3426.
- [9] Hung, P. K., et al. "Analysis for characterizing the structure and dynamics in sodium disilicate liquid." *Journal of Non-Crystalline Solids* 452 (2016): 14-22.
- [10] Jabraoui, H., E. M. Achhal, A. Hasnaoui, J-L. Garden, Y. Vaills, and S. Ouaskit. "Molecular dynamics simulation of thermodynamic and structural properties of silicate glass: Effect of the alkali oxide modifiers." *Journal of Non-Crystalline Solids* 448 (2016): 16-26.
- [11] Mountjoy, Gavin, Bushra M. Al-Hasni, and Christopher Storey. "Structural organisation in oxide glasses from molecular dynamics modelling." *Journal of non-crystalline solids* 357, no. 14 (2011): 2522-2529.
- [12] Jabraoui, Hicham, Yann Vaills, Abdellatif Hasnaoui, Michael Badawi, and Said Ouaskit. "Effect of sodium oxide modifier on structural and elastic properties of silicate glass." *The Journal of Physical Chemistry B* 120, no. 51 (2016): 13193-13205.
- [13] Voigtmann, Th, and Juergen Horbach. "Slow dynamics in ion-conducting sodium silicate melts: Simulation and mode-coupling theory." *EPL (Europhysics Letters)* 74, no. 3 (2006): 459.
- [14] Thao, N. T., et al. "Study of sodium diffusion in silicate glasses. Molecular dynamics simulation." *Modelling and Simulation in Materials Science and Engineering* 31.8 (2023): 085012.
- [15] Gupta, Y. P., and T. B. King. "Self-diffusion of sodium in sodium silicate liquids." *Transactions of the Metallurgical Society of AIME* 239, no. 11 (1967): 1701.
- [16] Braedt, M., and G. H. Frischat. "Sodium self diffusion in glasses and melts of the system Na₂O-Rb₂O-SiO₂." *Physics and chemistry of glasses* 29, no. 5 (1988): 214-218.
- [17] Knoche, Ruth, Donald B. Dingwell, F. A. Seifert, and Sharon L. Webb. "Non-linear properties of supercooled liquids in the system Na₂O-SiO₂." *Chemical geology* 116, no. 1-2 (1994): 1-16.
- [18] Meyer, A., J. Horbach, W. Kob, Florian Kargl, and H. Schober. "Channel formation and intermediate range order in sodium silicate melts and glasses." *Physical review letters* 93, no. 2 (2004): 027801.
- [19] Kargl, F., H. Weis, T. Unruh, and A. Meyer. "Self diffusion in liquid aluminium." In *Journal of Physics: Conference Series*, vol. 340, no. 1, p. 012077. IOP Publishing, 2012.

- [20] Jund, Philippe, Walter Kob, and Rémi Jullien. "Channel diffusion of sodium in a silicate glass." *Physical Review B* 64, no. 13 (2001): 134303.
- [21] Van, To Ba, P. K. Hung, L. T. Vinh, N. T. T. Ha, L. T. San, and Fumiya Noritake. "Network cavity, spatial distribution of sodium and dynamics in sodium silicate melts." *Journal of Materials Science* 55, no. 7 (2020): 2870-2880.
- [22] Konstantinou, Konstantinos, Dorothy M. Duffy, and Alexander L. Shluger. "Structure and luminescence of intrinsic localized states in sodium silicate glasses." *Physical review B* 94, no. 17 (2016): 174202.
- [23] Greaves, G. N. "Structure and ionic transport in disordered silicates." *Mineralogical Magazine* 64, no. 3 (2000): 441-446.
- [24] Greaves, G. N., and Sabyasachi Sen. "Inorganic glasses, glass-forming liquids and amorphizing solids." *Advances in physics* 56, no. 1 (2007): 1-166.
- [25] Khan, Mahfoozurrahman, et al. "Applications of polyaniline-impregnated silica gel-based nanocomposites in wastewater treatment as an efficient adsorbent of some important organic dyes." *Green Processing and Synthesis* 11.1 (2022): 617-630.
- [26] Khan, Mahfoozurrahman, et al. "Polyaniline modified silica gel coupled with green solvent as eco favourable mobile phase in thin layer chromatographic analysis of organic dyes." *Applied Chemical Engineering* 4.1 (2021): 41-55.
- [27] Mahfoozurrahman Khan "Preparation characterization and applications of polyaniline impregnated silica gel for the identification and separation of some important organics." *Thesis, Department of Applied Chemistry, Aligarh Muslim University, Aligarh, India* (2018): 1-158
- [28] Noritake, Fumiya. "Structural transformations in sodium silicate liquids under pressure: New static and dynamic structure analyses." *Journal of Non-Crystalline Solids* 473 (2017): 102-107.
- [29] Fábíán, M., P. Jóvári, E. Sváb, Gy Mészáros, Th Proffen, and E. Veress. Network structure of 0.7SiO₂-0.3Na₂O glass from neutron and x-ray diffraction and RMC modelling. *Journal of Physics: Condensed Matter* 19 (2007) 33, 335209.

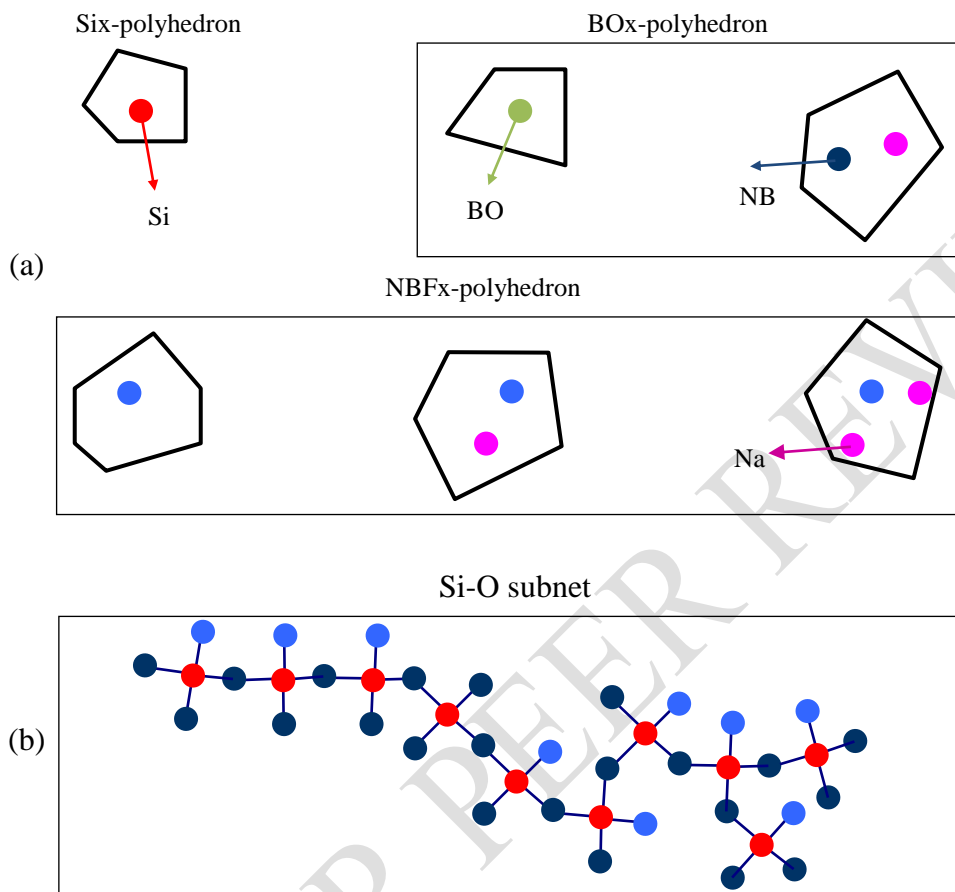


Figure 1. Schematic illustration of A_x -polyhedrons (a) and Si-O subnet (b). Here A is Si, BO or NBF; $x = 0, 1, 2, 3$ and 4. A_x -polyhedron can contain Na atoms.

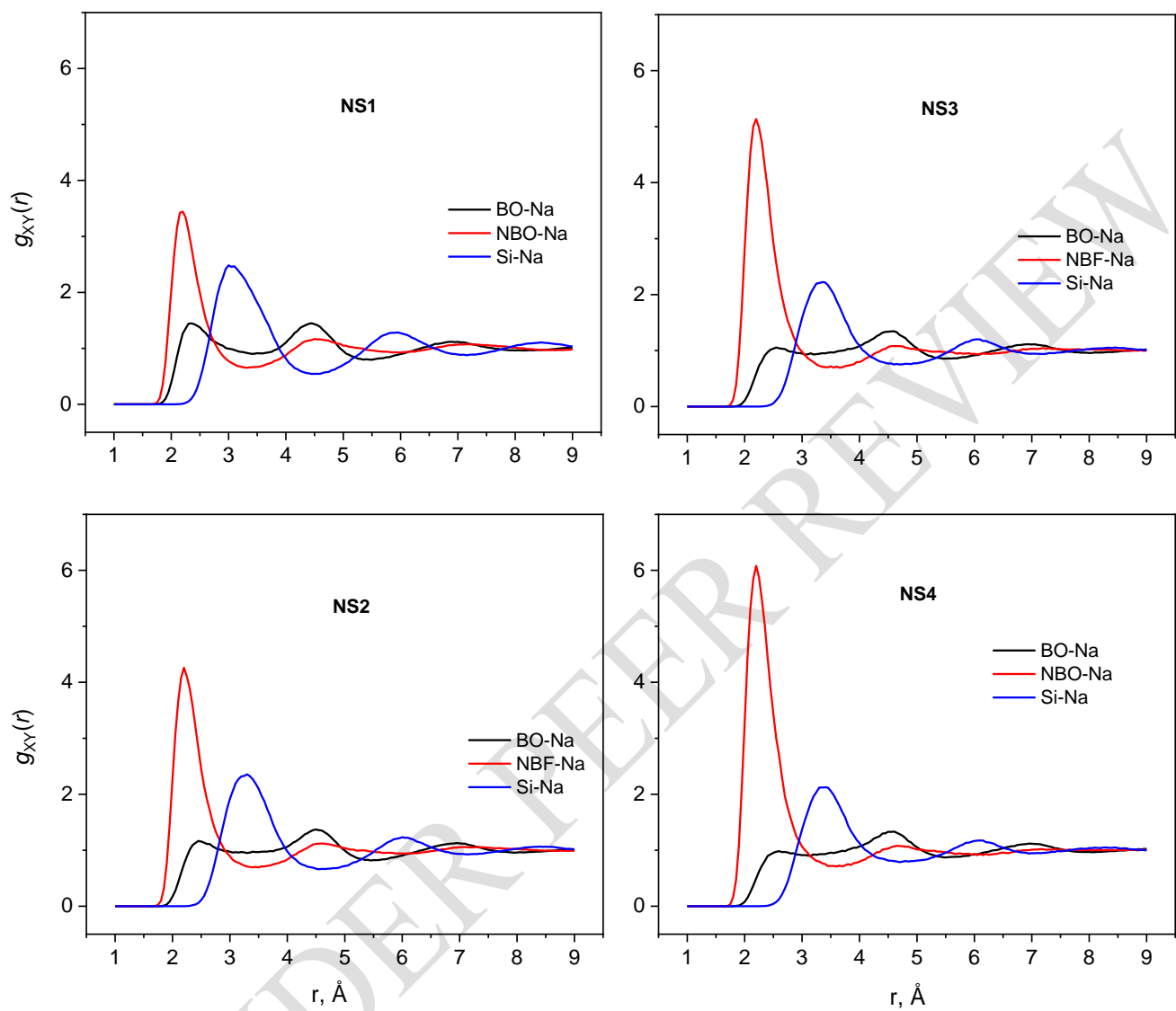


Figure 2. PRDF for NBF-Na, BO-Na, and Si-Na pairs of NSx at temperature of 1573 K and pressure of 0.1 MPa.

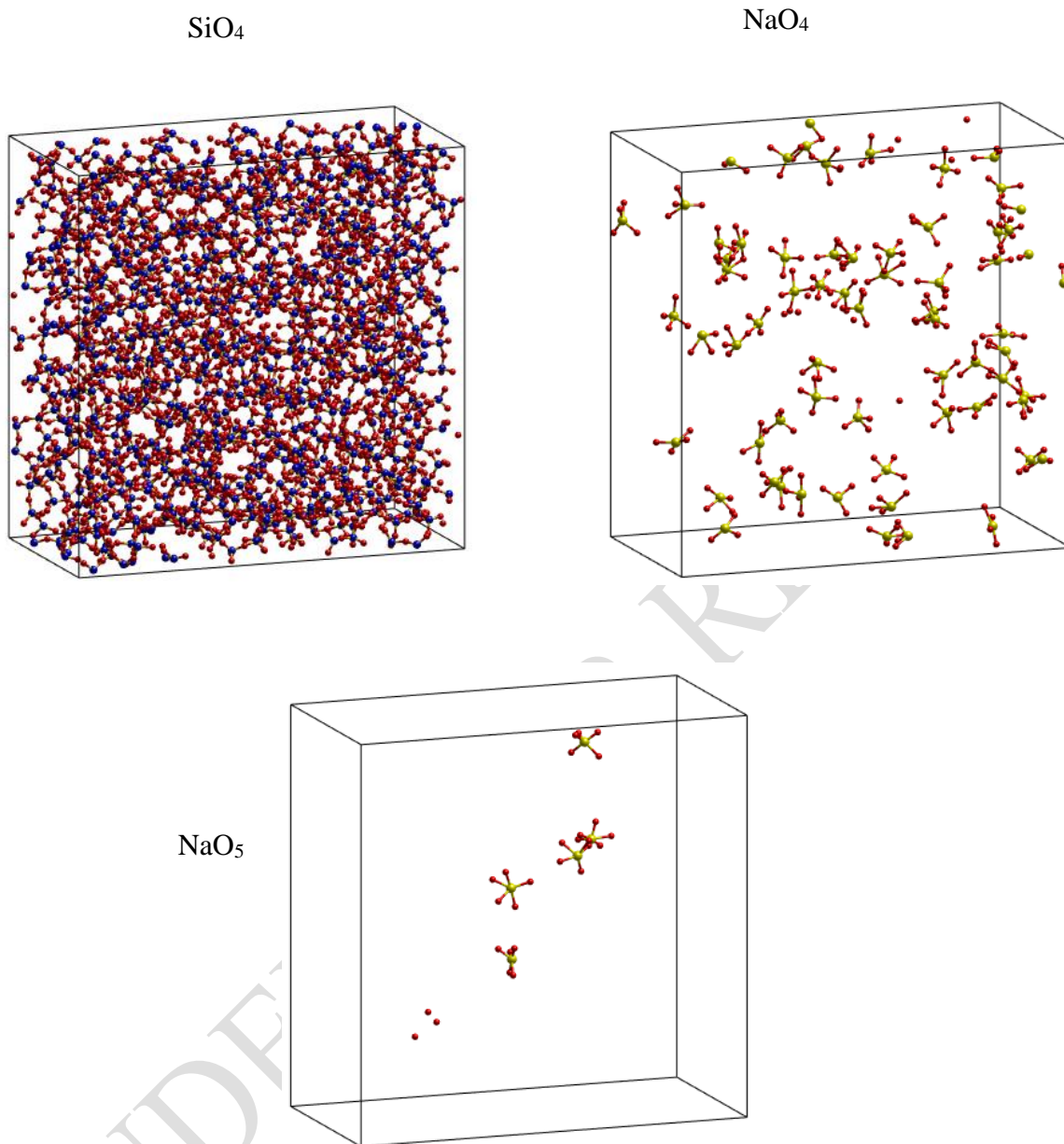


Figure 3. Spatial distribution of SiO_x and NaO_y in sample $\text{Na}_2\text{O}-3\text{SiO}_2$ at temperature of 1573 K and pressure of 0.1 MPa, here O (red color), Si (blue color), Na (yellow color).

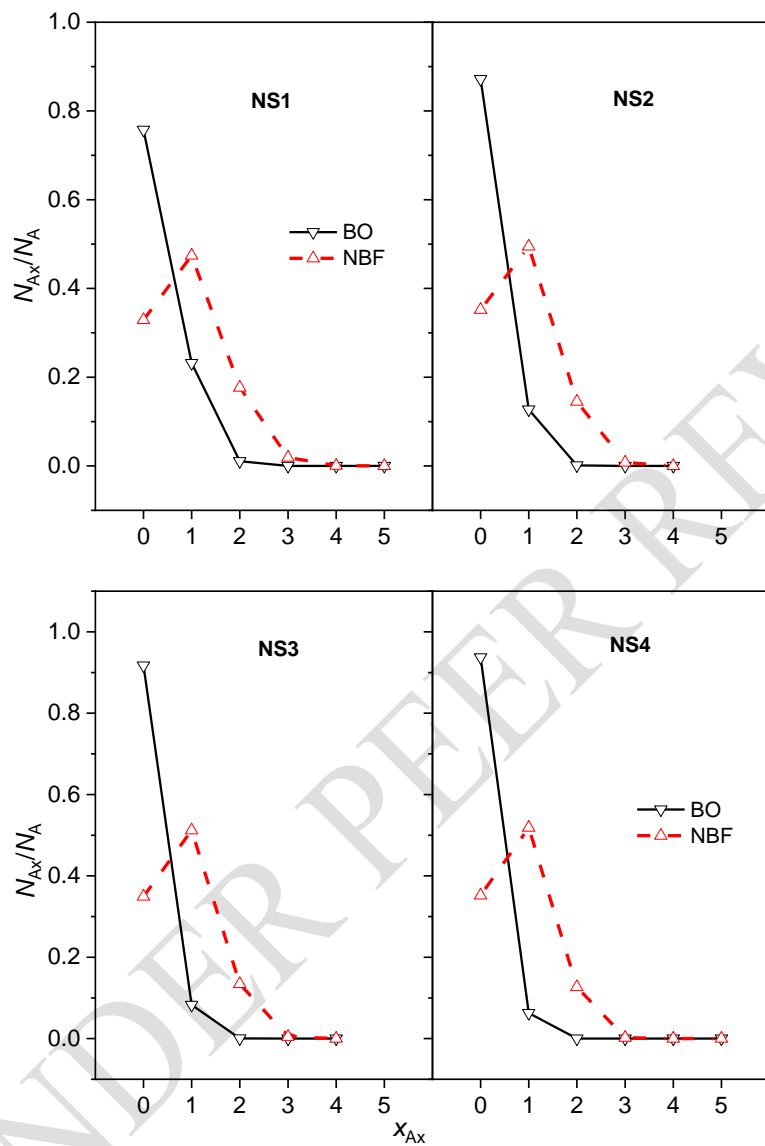


Figure 4. The fraction N_{Ax}/N_A as a function of x_{Ax} . Here N_{Ax} , N_A is the number of Ax -polyhedrons with x_{Ax} , and total number of A ; x_{Ax} is the number of Na in Ax -polyhedron; A is the BO or NBF.

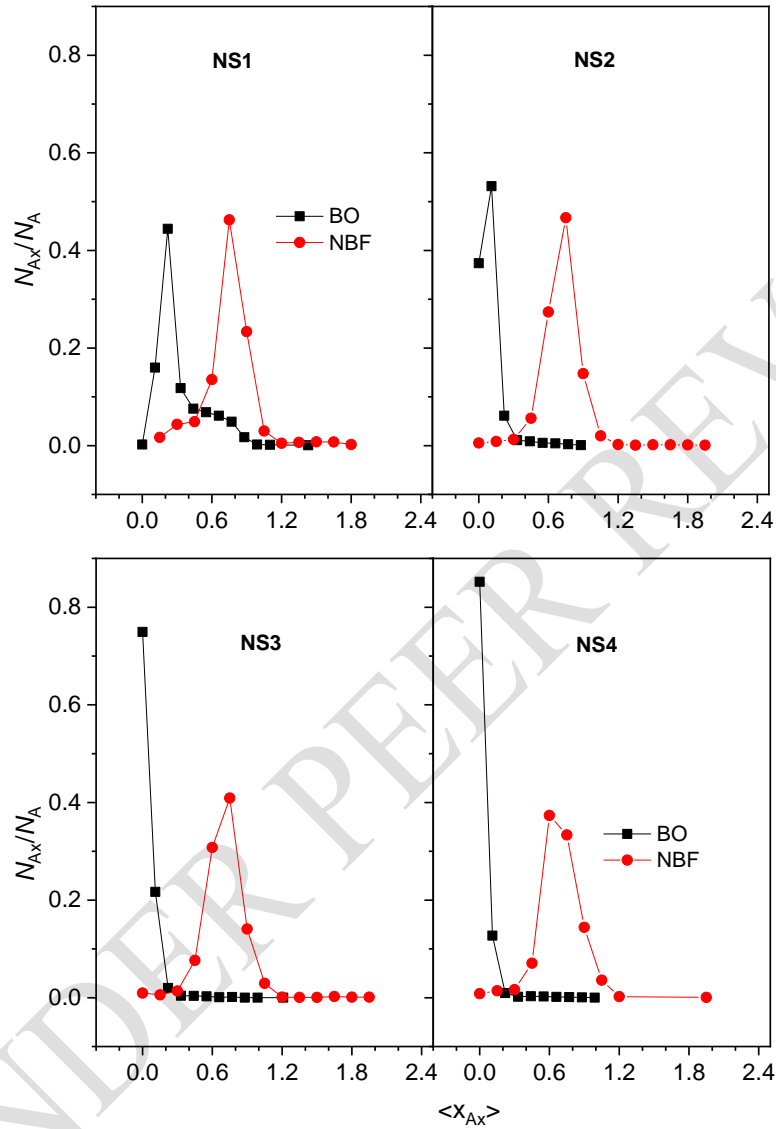


Figure 5. The fraction N_{Ax}/N_A as a function of $\langle x_{Ax} \rangle$. Here N_{Ax} , N_A is the number of Ax-polyhedrons with $\langle x_{Ax} \rangle$ and total number of BO or NBF; $\langle x_{Ax} \rangle$ is the average number of Na in Ax-polyhedron during 150 ps.